

Title – The behaviour of aluminium matrix composites under thermal stresses-a review

Authors – Khushbu Dash, Suvin Sukumaran, Bankim Chandra Ray

Author affiliations –

Corresponding author

Khushbu Dash
Research Scholar
Dept. of Metallurgical and Materials Engg.
National Institute of Technology,
Rourkela – 769008
Phone – +91-9439281130(M)
Fax - +91-661-2465999
E-mail – khushbudash@gmail.com

Co-authors

Suvin Sukumaran
M.Tech student
Dept. of Metallurgical and Materials Engg.
National Institute of Technology,
Rourkela – 769008
Phone – +91-7381500640(M)
Fax - +91-661-2465999
E-mail – suvin09@gmail.com

Bankim Chandra Ray
Professor
Dept. of Metallurgical and Materials Engg.
National Institute of Technology,
Rourkela – 769008
Phone – +91-9437221560 (M)
Fax - +91-661-2465999
E-mail – drbcray@gmail.com

The behaviour of aluminium matrix composites under thermal stresses-a review

K. Dash*, S. Sukumaran and B.C. Ray

Department of Metallurgical & Materials Engineering

National Institute of Technology Rourkela, Rourkela – 769008, India

Abstract

The present review work elaborates the behaviour of aluminium matrix composites (AMCs) under various kinds of thermal stresses. AMCs find a number of applications such as automobile brake systems, cryostats, microprocessor lids, space structures, rocket turbine housing and fan exit guide vanes in gas turbine engines. These applications require operation at varying temperature conditions ranging from high to cryogenic temperatures. The main objective of the paper is to understand the behaviour of AMCs during thermal cycling, under induced thermal stresses and thermal fatigue. It also focuses on the various thermal properties of AMCs such as thermal conductivity and coefficient of thermal expansion (CTE). CTE mismatch between the reinforcement phase and the aluminium matrix results in the generation of residual thermal stress by virtue of fabrication. These thermal stresses increase with increasing volume fraction of the reinforcement and decrease with increase in interparticle spacing. Thermal cycling enhances plasticity at the interface resulting in deformation at stresses much lower than their yield stress. Low and stable coefficient of thermal expansion can be achieved by increasing the volume fraction of the reinforcement. The thermal fatigue resistance of AMC can be increased by increasing the reinforcement volume fraction and decreasing the particle size. The thermal conductivity of AMCs decreases with increase in reinforcement volume fraction and porosity.

Keywords: Aluminium Matrix Composite: Thermal Stress: Thermal Cycling: Thermal Fatigue

*Corresponding author:

E-mail: khushbudash@gmail.com

Phone no: +91 661 2640369

1. Introduction

There has been a rapid growth in the development of metal matrix composites (MMCs) since the year 1960s due to variety of properties offered by it such as high specific strength, high specific stiffness, low density, good elevated temperature stability and good wears resistance [1]. Their commercial availability has also been increasing steadily and as a result information about the thermal properties of these materials is essential for the proper designing of MMC applications [2]. Among the metal matrix composites, aluminium matrix composites have drawn considerable attention in the academic and industrial sector recently. Improvement in strength and modulus has been reported for aluminium matrix composites over conventional metal alloys. This along with thermal stability makes them a good choice for use as materials in aerospace and transport industries [3]. The main property that makes MMC unique is that they offer a large variety of properties by means of combining possible combinations of matrices and the reinforcements, which in turn enables them to adapt the material properties according to the application requirements [4]. Using aluminium alloys as the matrix phase provides a large variety of properties such as low density, better corrosion resistance, good thermal and electrical conductivity, high damping capacity and ability to be strengthened by precipitation [5].

AMC finds applications in a number of structural, non-structural and functional applications in different fields of engineering, due to their economic, environmental and performance benefits. They are now being used in fabricating aerospace and automotive components such as ventral fins, fuel access door covers, rotating blade sleeves, gear parts, crankshafts, and suspension arms. In electronic industry they are used in the processing of integrated heat

sinks, microprocessor lids and microwave housing. Majority of these applications requires operation at varying temperature conditions ranging from high to cryogenic temperatures [6, 7]. Structural components used in the aerospace industries such as aircraft wings, fuselage frames and landing gears are frequently exposed to severe thermal loads created by aerodynamic heating [8,9]. Hence, it is important to study their thermal behaviour under these conditions.

The ceramic phase which is generally used as reinforcement in MMC has a large difference in coefficient of thermal expansion with the metal phase. This thermal mismatch causes large residual thermal stresses near the interfaces of composite when they are cooled from the fabrication temperature [10, 11]. These residual stresses have a significant influence on the mechanical and physical properties of the composite. Thermal stresses are important in design because they lead to plastic yielding or failure of the material [12]. There are several mechanisms by which thermal stresses can be relaxed which includes interface debonding, by micro plasticity of the metal matrix and crack initiation and propagation [13]. Aluminium matrix composites are frequently being exposed to environments where cyclic temperature changes prevail [10]. Thermo-mechanical cycling also greatly influences the thermal expansion behaviour of the composites [14]. Studying thermal expansion behaviour of composites also have significant importance since most of the structural components are subjected to variable temperature operation and hence the materials used in these components should have lower and stable CTE and outstanding mechanical properties [3]. Thermal expansion behaviour of composites is affected by several material parameters such as the type of constituents, matrix microstructure, reinforcement volume fraction and architecture, the internal stresses due to their CTE mismatch, thermal history, porosity and interface bond strength [9].

Thermal fatigue study of aluminium matrix composites become important since they are used in engine components which are subjected to thermal excursions during service such as piston crowns and valves [15]. It is also important to understand the properties like thermal conductivity of MMC for various thermal management applications such as heat sinks in electronic devices, microprocessors, power semiconductors, high-power laser diodes, light-emitting diodes (LEDs), and micro-electro-mechanical systems (MEMs) [16,17]. This paper reviews the current knowledge on the behaviour of aluminium matrix composites under thermal stresses.

2. Classification of metal matrix composites

There are mainly four types of metal matrix composites based on the type of reinforcement such as:-

- i. Particle reinforced MMC: These are produced by incorporating equiaxed reinforcements in the form of particles to the metal matrix. The aspect ratio of particles will be less than 5 and are less expensive compared to other reinforcement types. But the mechanical properties of particulate reinforced MMCs are less compared to that of whisker and fibre reinforced MMCs. These composites are usually isotropic in nature and manufactured mainly by powder metallurgy processing. Secondary forming operations such as rolling, forging, extrusion etc can be performed easily on particulate reinforced MMCs.
- ii. Short fibre and whisker reinforced MMC: Here non continuous fibres with an aspect ratio greater than 5 are used. Whisker reinforcements have better mechanical properties than both continuous and particles reinforced composites and are mainly fabricated using powder metallurgy or squeeze infiltration route. Short fibre reinforcements find major application in use as piston and have intermediate

properties in between that of continuous fibre reinforced MMCs and particulate reinforced MMCs. Since some health hazards are identified with use of whisker as reinforcement, their commercial applications have been limited lately.

- iii. Continuous fibre reinforced MMC: Continuous fibres are used here which can be parallel or pre woven. They have diameter normally less than 20 μ m. The highest degree of load transfer is provided by them due to their high aspect ratio. Significant amount of strengthening takes place along the fibre direction. Liquid infiltration techniques are mostly employed for the fabrication of continuous fibre reinforced MMCs. But the main disadvantage of these composites is that they have low strength in the transverse direction compared to the longitudinal direction which results in anisotropic properties.
- iv. Mono filament reinforced MMC: Here fibres having large diameter in the range 100-150 μ m, are used as reinforcements. Chemical vapour deposition and diffusion bonding techniques are normally used for their fabrication. Their application is limited to superplastic forming metal matrices. Like continuous fibre reinforced MMCs, these composites also have anisotropic properties.

In addition to the above types, another variant called hybrid AMC's having more than one type of reinforcement are also present, which are in use to some extent [6,18,19].

3. Synthesis of aluminium matrix composites

Primarily fabrication of MMCs can be classified into two processes such as solid state processes and liquid state processes. Solid state processes include powder metallurgy process, diffusion bonding and deposition process. Powder metallurgy is generally used for the fabrication of particulate reinforced aluminium matrix composites which involves blending, cold pressing and sintering, or hot pressing. For obtained a near net shaped final product,

powder forging technique can be used where forging operation is done after the sintering stage. Diffusion bonding is another solid state process for MMC fabrication where interdiffusion of atoms between metallic surfaces take place at high temperatures leading to bonding. It can be used for production of mono filament-reinforced AMCs through either foil-fibre-foil route or by evaporating thick aluminium layers onto the fibre surface. This process is not suitable for obtaining high volume fraction of fibres and obtaining complex shapes. Also, long processing time and high temperature requirements limits the commercial applicability of the process.

Various deposition techniques are available for MMC production which includes spray deposition, physical vapour deposition (PVD) and chemical vapour deposition (CVD). Physical vapour deposition process can be used for the fabrication of multilayered MMCs in the nanometre range by passing the fibres continuously through a region of high partial pressure vapour of the metal to be deposited. Here condensation takes place which results in a relatively thick coating of metal on the fibre. Spray deposition technique involves spraying the molten metal onto winded fibres to form the composite. Rapid solidification of molten matrix and easier control of fibre alignment are the main advantages of spray deposition. The decomposition of vaporised metallic component onto the substrate fibre at elevated temperature constitutes the chemical vapour deposition technique (CVD). The ease of controlling the degree of interfacial bonding is one of the key aspects of deposition processing. The main problem with deposition technique is that they are very time consuming processes.

Liquid state processing involves stir casting, infiltration techniques and spray deposition process. In Stir casting technique, the ceramic particles are first added to the molten metal and then it is allowed to solidify. Proper wetting between the reinforcement and the molten metal is an important criterion which determines the mechanical properties of the final

product. One of the main problems with this technique is that reaction between the fibre and the matrix may take place which can deteriorate the properties of the composite. Compo casting is another variant of stir casting where the particles are incorporated to the matrix alloy in the semi solid state. A fibre or particulate preform is being infiltrated by using molten metal for the producing the composite in the case of infiltration technique. Here minimal reaction takes place between the matrix and the reinforcement due to shorter processing period involved. Gas pressure infiltration is another variant of liquid infiltration technique where the fibre preform is being infiltrated by using a high pressure inert gas. In spray forming process the composites are produced by injecting the ceramic particles into an atomized spray of molten metal matrix. Even though expensive compared to other processes, this fabrication route is very flexible and here no harmful reaction products are formed since the time of flight of composite particles is very less [6,18,19].

4. Thermal Stresses

Under uniform temperature change, thermal residual stresses are induced in a composite due to thermal expansion mismatch between the matrix and the reinforcing phases. These stresses are important as they exist at room temperature and can decrease the initial yield stress, relative to its value in the absence of internal stress. Even though a small strain mismatch can be accommodated elastically; the entire deformation volume of a MMC may become plastically deformed for larger strain mismatch [10-12,20]. For Al-based metal matrix composites, it has been reported that dislocations are generated at the reinforcement–matrix interfaces to provide sufficient space for the strains originating from the coefficients of thermal expansion (CTE) mismatch between the Al matrix and the ceramic reinforcements and the internal stresses resulting from this mismatch are being partially relaxed by these dislocation processes [21-23]. These residual thermal stresses can accelerate creep by orders

of magnitude and when their average value exceeds the externally applied stress, they will play a significant role in the determination of plastic deformation rates. When average thermal stresses within a composite become similar to (or greater than) the externally applied stresses, the thermal stresses will have an important (or dominant) role in determining plastic deformation rates [24].

Even though experimental determination of residual stress in composites is possible through XRD [25], dilatometry and acoustic methods; difficulties arise in measurement which includes lowering original value of residual stress due to relaxation processes taking place. Original residual stresses can be ascertained by the comparison of stress/strain curves of the matrix and the fibre. Generally during the fabrication of composites, a tensile residual stress is developed in the matrix which accelerates the change in deformation from elastic to plastic in matrix whereas a compressive residual stress is generated in the fibre which slows the transition. This transition occurs when the residual stress in the matrix exceeds the yield strength of the matrix. During the prestraining of composite, residual stresses are formed in the fibre and the matrix which also depends on the value and sign of original residual stress [26]. Premature yielding during axial loading and yielding prior to loading occurs due to the generation of residual stress in the composites.

During cooling of a composite from fabrication temperature there are three different stages of matrix deformation. In the first stage occurring at high temperatures, there will be negligible amount of residual stress build up in the matrix due to stress relaxation. The temperature at which first stage ends depends up on the cooling rate employed. In the second stage as temperature lowers further, the residual stress build up begins in the constituents rapidly and when the value of residual stress is large enough to exceed the yield strength of the matrix, plastic deformation occurs in the matrix which marks the beginning of third stage. In the case of graphite fibre reinforced aluminium matrix composites there exists anisotropy in the

coefficient of thermal expansion of graphite fibre (0°C^{-1} in longitudinal direction and $25 \times 10^{-6} \text{ }^{\circ}\text{C}^{-1}$ in transverse direction) which results in larger residual stress in the longitudinal direction compared to the transverse direction. This anisotropy in thermal expansion is beneficial as it along with slow cooling rate can eliminate the plastic deformation in the matrix created due to coefficient of thermal expansion mismatch [25, 27-29]. Volume fraction of graphite fibres also play a significant role in deciding the magnitude, sign and distribution of residual thermal stresses [30].

The effect of modifying the residual thermal stress in a graphite fibre reinforced aluminium matrix composite by tailoring the interfacial region was observed to depend on the elastic modulus of the interfacial region. A larger elastic modulus resulted in increasing the contribution of matrix-interfacial region mismatch terms which is very harmful to the thermal stresses in aluminium matrix composites as it increases tensile hoop stresses during cooling from processing temperatures [31]. The overall yield surfaces of the particulate reinforced composites such as SiC/Al exhibit a combination of kinematic and isotropic plastic hardening due to the presence of thermal residual stresses [32].

In the majority of the earlier investigations, the residual thermal stresses were determined using either Eshelby Method or Finite Element Method [22]. Eshelby model was used for the prediction of thermal residual stress in SiC whisker reinforced aluminium composites which were in good agreement the experimental results [33]. In the case of SiC short fibre reinforced aluminium system it predicts the resultant stress distribution between the phases. The relaxation of thermal residual stresses occurs commonly through mechanisms such as general plastic deformation (plasticity, creep), fracture (fibre cracking, interfacial decohesion, interface gliding), local plastic deformation (dislocation glide) and diffusion (atom movements) which affect the stress contributions in many ways. Generally residual stresses can be relaxed during cooling at high temperatures, but at low temperatures relaxation is very

difficult to take place. But there exists complexity in Al/SiC system where relaxation of residual stresses occurs even after it is cooled down to the room temperature [34,35].

High density of matrix dislocations was observed near the interface in SiC/Al system created due to residual stress and these dislocations are emitted from the interface. The effect of aspect ratio of SiC fibres on thermal stresses is very little because at short distances from fibre corner, the dependence of residual fields on the axial position is negligible. But side to side fibre spacing has a profound influence on the magnitude and distribution of residual stress in the fibre and on the interfacial stresses at whisker end. As side to side fibre spacing was increased greater plastic strains were observed on the fibre corner [36]. Thermal residual stresses have very little direct influence on the predicted ductility of the SiC_f/Al system even during the case when the limiting failure mechanism in modelling the system was assumed to be void nucleation by interfacial debonding at the whisker ends. There is a tendency for redistribution in residual stresses as interface failure begins to occur. Flow strength in compression was observed to be greater than that in tension when a closer end to end spacing of fibres was maintained [37].

The various factors on which the magnitude of thermal residual stress depends includes coefficient of thermal expansion of fibre and matrix, their elastic properties and matrix-plasticity behaviour. In a unidirectional SiC fibre reinforced 6061 aluminium alloy, the amount of age-hardening produced is significantly less than that in the bulk alloy due to the plastic strain brought about during cooling. Solute migration tendency to fibres as well as to strain induced dislocations may enhance this effect. Stress relaxation behaviour in the matrix of the composite is more intricate than that of normal stress relaxation. Due to the elastic constraint imposed onto the matrix by the fibres, plastic strain due to stress relaxation will create a decrease of elastic strain in both the fibre and the matrix. [38,39]. Analysis of the influence of thermal residual stresses and strains on the mechanical behaviour of Al₂O₃

particulate reinforced 6061-T0 Al alloy through finite element method pointed out that the residual stress/strains have large influence on composite behaviour under compressive loading than tensile loading. Also when the residual thermal stresses/strains are introduced prior to external loading, there was a decrease in proportional limit, 0.2% offset yield stress and the apparent stiffness. Regions of constrained plasticity and high stress triaxiality in the matrix around the particle help in better load transfer in the composite [40].

Increased matrix dislocation density as a result of differential thermal contraction is the main strengthening mechanism observed in discontinuously reinforced MMCs such as SiC/Al. Various undesirable composite properties are caused by thermal stresses such as lowering of tensile and yield strengths, elevating Bauschinger effect affecting load transferring capability of the matrix to the fibre. Residual stresses can enhance interface strength in the case of composites with weak interfaces during tensile loading, which is more prominent in regions of plastically deformed matrix near the interface [41,42].

Average strain in aluminium matrix composites components resulting from thermal stress can be determined by using neutron diffraction and synchrotron techniques. An equivalent inclusion method helps in interpreting these thermally induced lattice strains [20,43-45]. The effect of thermal stress on the microstructure of Al-metal matrix composites reinforced with nanosized dispersoids of mullite and zirconia fabricated using uniaxial hot-pressing was studied at three different temperatures in the range of 450°C to 610°C. Through the analysis an estimation of the thermal stress of the AMCs using analytical functions was made possible. The results revealed that magnitude of the thermal stress increased with the increase of processing temperature. As a result the Al matrix was deformed to the extent that the effective particle sizes of the matrix decreased, strains increased and the values of dislocation density increased with increasing processing temperatures which lead to the betterment of hardness and mechanical properties of the composites [46]. Analysis using FEM models

depicted that thermal stresses cause pronounced matrix yielding during axial tensile loading and elevates flow stress during transverse tension in unidirectional boron fibre reinforced 6061 Al alloy composite. However, local spacing of the fibres also influences the local magnitude and sign of the residual stress in the matrix [47].

In the case of discontinuous SiC whisker reinforced aluminium-matrix composites, it was observed that residual stresses significantly affects the constrained matrix plastic flow and matrix-fibre load transfer which were the main strengthening mechanisms. The effect of thermal residual stress on load transfer was found to be increasing with the whisker volume fraction. Thermal residual stresses were found to delay void nucleation in the matrix and interfacial decohesion at the fibre-ends during tension at lower whisker volume fraction. This was attributed to the induction of hydrostatic compression in the interfacial region of the composites. But at higher volume fraction they aids matrix and/or interfacial damage in the fibre –ends under tensile loading [48]. In SiC particle reinforced aluminium matrix fabricated by casting, residual stress distribution was observed to be increasing with the cooling rate. Elastic modulus and yield strength of the composite was increased due to the residual thermal stress formation. The value of residual stress was higher at the interface and decreases with distance from the interface. Interface stresses are strongly influenced by the thermal residual stresses when mechanical loading is applied. Residual stresses was found to be increasing with the volume fraction of the fibres in the heat removal direction and the direction normal to it for air-cooling and water-cooling but for constant temperature cooling, they remained approximately same for different volume fractions in the heat removal directions and decreased with volume fraction of fibres in other directions [49-51]. In a nickel coated-carbon fibre reinforced aluminium matrix composite, thermal stresses arising due to temperature gradient resulted in the failure of nickel coating [52]. Thermal residual stresses were

significantly reduced by using a thermal expansion clamp during curing in the case of a carbon fibre reinforced aluminium laminates (CARALL) [53].

A twofold effect of pressure rolling on the residual stresses were observed on the residual stress state of a SiC particle-reinforced 2014 aluminium alloy which was investigated by using a modified Eshelby model [54]. The residual stresses induced by annealing in silicon carbide particle reinforced aluminium metal matrix composite measured using x-ray diffraction method indicated that hydrostatic tension was developed for aluminium matrix and hydrostatic compression was developed for the SiC reinforcement which established force equilibrium making the macroscopic thermal stress absent in the composite. But when the composite was subjected to grinding treatment, the thermal stresses were reduced and resulted in a macroscopic stress such that compressive stresses were measured in both the constituents [55]. Tensile stress distribution due to the rotation of aluminium based composite disc containing silicon carbide whisker was changed significantly due to the presence of residual stress. The steady state tensile creep rate was further enhanced by the tensile residual stress which may lead to decrease in the service life of component which finds major applications in flywheel, shrink fits and turbines [56,57]. When the stiffness of a composite material is increased it will also obstruct thermal expansion which in turn will lead to higher residual thermal stresses whose maximum along the axial direction occurs in the boundary of elastic and plastic zones [12].

In the finite element method analysis of the distribution and the amount of residual stresses in the SiC particle reinforced aluminium matrix, carried out recently by Bouafia et al. [58], large amount of residual thermal stresses were generated, mostly at the interface region of the composite. The SiC particles volume fraction and interparticle spacing plays prominent role in the production of residual thermal stresses. Lowering SiC particle volume fraction and increasing interparticle spacing resulted in the decrease of internal residual stresses and vice

versa. SiC particles with cylindrical shape developed higher thermal stresses compared to those with spherical and cubical shape. Increasing the reheating temperature also resulted in the increment of normal internal stresses introduced in the matrix and the particle.

Thermal residual stresses are one of the main causes of interface damage and fatigue crack initiation during high-cycle fatigue in alumina reinforced aluminium matrix composites. Surface treatment capable of inducing compressive residual stresses can be done to improve the fatigue behaviour of composite by preventing the crack propagation in the initial stage itself [59]. The relaxation of thermal stresses in aluminium-based MMCs subjected to thermal cycling was studied using mechanical spectroscopy where the mechanical losses and shear modulus measurements were taken as a function of temperature. When the composite was cooled, maximum mechanical loss appeared because of the dislocation generation and motion near the interfaces due to differential thermal contraction of matrix and reinforcement. This mechanical loss maximum is absent in the case of monolithic material. Also, when the reinforcement volume fraction was increased, the maximum mechanical loss was found to be increased [60]. The change in residual stress on heating and cooling of the magnesium borate whisker-reinforced aluminium composite was investigated using coefficient of thermal expansion (CTE) curves, where a close relationship was observed between the CTE of the composite and the residual stress changing rate. A linear relationship was observed on tensile and compressive stress changing rates with temperature while heating the matrix at lower and higher temperature ranges. The CTE of the composite on cooling was found to be smaller than that on heating. This is because while heating, the residual stress present in the Al matrix is elastically relaxed in lower or higher temperature region [61].

5. Thermal Cycling

In the case of AMCs, heat treatment has been widely used as an effective technique for acquiring stabilized microstructure and best achievable properties. Thermal cycling is one

among the effective heat treatment methods to reduce residual stresses and improve dimensional stability of the composite which involves alternatively cooling and heating the material to improve its strength and capacity [8]. Information on stress relaxation mechanisms can be obtained from the in-cycle creep data for metal matrix composites subjected to thermal cycling which are essential in life prediction of structural components under thermal cyclic environments [62,63].

During thermal cycling conditions, the strain rate sensitivity exponent (m) of the composite material is unity (Newtonian flow behaviour) since the strain rate will be proportional to the applied stress and at higher stresses the material gradually approaches the isothermal flow behaviour of the matrix. The internal stresses which block or assist the motion of individual dislocations are the main cause for thermal cycling behaviour [64]. During thermal cycling, shape instabilities and creep at significant strain rates are observed in metal matrix composites, even at unusually low stresses [65,66]. Densification of composites also increases during thermal cycling under stress. Thermal cycling of a material can be used to induce internal stress in many ways such as (1) thermal cycling of a material through a phase change while applying a small external stress; (2) thermal cycling of polycrystalline pure metals or single phase alloys with anisotropic coefficients of thermal expansion with simultaneous load application and (3) thermal cycling of composite materials in which constituents have different coefficient of thermal expansion [67].

The behaviour of metal matrix composites will be different from isothermal conditions when they are subjected to temperature cycling. Strain rate increases substantially even at lower temperatures during thermal cycling when compared to isothermal conditions. Fracture strain is also high during thermal cycling. Damage modes occurring during thermal cycling such as fibre and interface cracking, interface void formation may not necessarily occur during isothermal conditions [10,68]. Plastic flow stress and strain hardening behaviour of the

composites are affected by thermal cycling because of the triaxial state of stress generated at the particle–matrix interfaces. Residual stress can also have a considerable influence on the composites subjected to thermal cycling as they can initiate matrix phase yielding which causes the formation of strain hysteresis loops between the heating and cooling segments of the cycle. Large percentages of plastic deformation, known as internal stress superplasticity (mismatch induced superplasticity [65]) occurs in Al-SiC particulate composite when they are subjected to concurrent application of small external stress and thermal cycling [11]. Studies show that enhanced creep deformation is observed during the thermal cycling of particulate reinforced metal matrix composites and plastic strain per thermal cycle varies linearly with the applied stress [69].

When the displacement measurements within the graphite fibre of a graphite fibre reinforced aluminium matrix composite during thermal cycling was studied using in-situ SEM experiments, intrusion/extrusion phenomenon was observed which limits the matrix to fibre load transfer across the interface. Once shear begins within the graphite fibre, this phenomenon will further lead to modification of CTE of the composite [70]. Superplastic behaviour was observed at very low stresses (~ 10% of the yield strength) in SiC_p/Al composite when it was subjected to thermal cycling on a conventional creep machine at relatively low temperatures(<200°C) [64]. A drastic strength decrease is observed for SiC_w/Al system when they are subjected to thermal cycling in which plastic flow occurs and this effect limits the use of these materials in high temperature applications [71].

Thermal cycling can result in the generation of internal stresses at SiC_w/Al interfaces which are produced due to the CTE mismatch between SiC whiskers and aluminium matrix. The deformation produced due to these internal stresses results in superplastic behaviour leading to very high ductility of the composite (> 1000%) and thus high strain rate sensitivity. Also the rate of realignment and redistribution of whiskers are increased as a result of increase in

stress during thermal cycling [72]. The influence of thermal cycling on the precipitation events in a SiC whisker reinforced aluminium alloy matrix composite was studied by Hall et al. [68] at higher temperatures. A dispersion of finer precipitates was observed during thermal cycling in addition to the coarser precipitates and large dimensional changes were noticed.

Neutron diffraction techniques and X-ray synchrotron measurements were found to be useful for measuring internal strain changes in SiC whisker reinforced aluminium matrix composite undergoing thermal cycling [73-75]. Formation of stable dislocation tangles and cells were observed near the interface regions during thermal cycling of 10 vol% alumina particulate reinforced 1060-aluminium matrix composite [76]. Internal stresses resulting from CTE mismatch between the matrix and the particulates are partially relaxed by such dislocations [77]. Creep acceleration and reduction in creep stress exponent was reported [78] in the theoretic model of aluminium reinforced with SiC particles, which was subjected to thermal cycling under load. This further resulted in superplastic deformation behaviour with extensions in excess of 150%. The roughness of squeeze-cast aluminium matrix composite reinforced with 15 vol% random discontinuous saffil fibres subjected to thermal cycling was found to be increasing with the number of thermal cycles and increased dislocation density was observed at the interfacial region [79]. The damage mechanisms at the fibre-matrix interface are the chief factor contributing to the enhanced non-linear strain accumulation associated with thermal cycling [80].

A comparative study was made on the damage in three discontinuously reinforced aluminium matrix composites produced by powder metallurgy route such as Al-Mg-Cu alloy-SiC (as extruded and solution treated), Al-SiC(hot rolled) and in-situ cast Al-TiC (as extruded) composites. The matrix and interfaces in the Al alloy-SiC composite show cracks as a result of repeated thermal cycling because of the stress generated from the mismatch in CTE. This leads to a decrease in the Young's modulus of the composite and matrix micro

hardness near the particle-matrix interfaces. But increase in microhardness of the interface by strain hardening due to dislocation generation was observed as shown in Fig.1 in the case of as-rolled Al-SiC and in-situ Al-TiC as their interfaces are very strong so that no decohesion takes place. Also there was only marginal decrease in Young's modulus in these composites. Bar charts depicting the damages caused by thermal cycling in the Al alloy-SiC, Al-SiC and Al-TiC composites against the number of cycles of heating and water quenching are shown in Fig.2 [81].

The phenomenon where progressive plastic deformation with increasing number of thermal cycles occur in composites even at stress level far below the yield strength is known as thermal ratchetting which is a function of both the applied stress and the amplitude of thermal cycles. Thermal ratchetting behaviour has been observed in SiC_f/Al composites [82] and in C/Al and SiC/Al laminated composites [83]. Ratchetting rate is not influenced by highest temperature of the thermal cycle but it plays a prominent role in composite failure at high load levels. Progressive reduction in length was observed during repeated thermal cycling of saffil fibre reinforced aluminium matrix composites until a steady state cycle is reached [84]. Thermally activated recovery by polygonization was the major microstructural damage mechanism involved with thermal cycling at elevated temperature, as observed in the case of a short alumina silicate fibre reinforced aluminium alloy (A356) composite fabricated by pressure casting. Reduction in residual stresses was observed in Al₂O₃ fibre reinforced Al matrix and SiC whisker reinforced Al matrix during thermal cycling. This effect was mainly due to the thermally induced plastic relaxation and the degree of reduction depends on the difference in CTE between the constituent phases, volume fraction of the reinforcement and drop in temperature [85,86].

A study on the effect of strain control and thermal cycling on Aluminium alloy (AA6061) reinforced with alumina particles produced by casting and extrusion pointed out that thermal

stresses produced by thermal cycling can increase the plasticity at the matrix/reinforcement interface whose maximum exists at an optimum strain-rate condition. A comparison was made on the elongation of the composite with unreinforced AA6061 and re-extruded 6061 composite under room temperature, isothermal and thermal cycling conditions which are represented in the bar chart (Fig. 3) shown below [3]. Loading under thermal cycling does not change the dislocation density in the work hardened zone of short fibre reinforced aluminium matrix composites once cyclic saturation is achieved. Also, the dislocation loop punching that occurs during thermal cycling at high applied stresses acting for a short period of time is mainly controlled by dislocation glide mechanism [87].

Thermal cycling tests carried out on unidirectional Mo-fibre reinforced aluminium composites showed reduced tensile strength due to the presence of interfacial cracks which are generated to relax the internal stress built up in the composite. When the thermal cycles are increased, the axial length also increased but the density got reduced. The interfacial reaction between Mo-fibre and Al matrix is unimportant after thermal cycling as the Mo fibres remained intact [88]. During thermal cycling, strain hysteresis was observed in Al-12wt% Si alloy matrix composite reinforced with potassium titanate whiskers fabricated by squeeze casting process. Furthermore, the composite exhibited little dimensional change due to the absence of residual plastic strain [89]. A theoretical model based on micromechanical approach was developed by Dutta [90] for examining the thermal cycling behaviour of continuous graphite fibre reinforced aluminium matrix composites. From the analysis it was concluded that the influential deformation mechanism functioning in the matrix changes frequently during thermal cycling as a result of continuous stress and temperature revision. Overaging, matrix annealing, void coalescence, crack formation and reinforcement debonding were observed in SiC whisker reinforced 6061 aluminium matrix composite subjected to thermal cycling at beginning of T6 tempering treatment. Due to these defects, the

tensile strength, yield strength, Charpy impact energy and the fracture toughness of the composite was significantly reduced [91].

The maximum residual stresses were found to be generated at the interfacial region during the thermal cycling of 10 vol% SiC reinforced aluminium-silicon alloy matrix composite [92]. Also crack formation was observed in SEM micrographs under repeated action of thermal cycling process. The development of strain hysteresis loops was observed in aluminium-based composites reinforced with in-situ Al₃Ti plate and Al₂O₃ particles produced by reactive hot pressing method, which were exposed to fluctuating temperature environments [11]. Thermal damage of composites subjected to practical thermal cycling conditions can be assessed by thermal strain parameters deduced from the hysteresis loop and it was observed that in-situ composites displayed better dimensional stability compared to Al during thermal cycling which are mainly attributed to the higher thermal stability and improved interface bonding of in-situ reinforcements. The mechanical strength of graphite fibre reinforced aluminium composites produced by gas pressure infiltration method was reduced by 10% due to thermal cycling between 60°C and 300°C upto 1020 cycles. There was no effect of thermal cycling on the thermal conductivity of the composite [93]. The mechanical properties of AlN_p/Al composite fabricated by squeeze casting were greatly enhanced after thermal cycling treatments. Tensile strength of the composite was mainly improved by wide-range thermal cycling treatment whereas stability of material properties was improved by narrow range treatment. Moderate-range cycling treatment was found effective in improving yield strength and elastic limit. The elastic modulus of the composite was also significantly increased to as near as die-casting condition in moderate range and narrow range thermal cycling treatments [94].

High dislocation density was observed in the cast aluminium alloy matrix composite reinforced discontinuously with fine SiC particulates during thermal cycling, which can be

attributed to the difference in coefficient of thermal expansion of the constituents [95]. The internal friction of Al/SiC particulate MMC was increased by thermal cycling which is mainly due to the dislocation motion. Thermal cycling also caused increase in the dislocation density, which enhanced the damping capacity of the composite [96]. Reduction in hardness after thermal cycling was observed in short fibre reinforced AlSi12CuMgNi piston alloys which can be attributed to overaging and matrix recovery [97]. The thermal cycling of extruded aluminium–silicon alloy (Al–7% Si–0.7% Mg) based composites reinforced with particulate silicon carbide displayed higher ductility mainly due to internal stresses which are being generated as a result of CTE mismatch between the matrix and the reinforcement. Thermal cycling caused the matrix alloy and its composites to deform at stresses much lower than the yield stress. Formation and transversal growth of the cavities was found to be the dominating factor in the failure of thermally cycled composites which are present along the gauge leading cracks in the matrix in the transverse direction to the applied stress as observed in the Fig.4 below [14,98].

A constant and higher strain rate compared to pure creep conditions was observed in the deformation behaviour of an aluminium alloy matrix composite reinforced with SiC particles during thermal cycling between the temperature limits of 305K and 443K. The enhanced deformation taking place in the thermally cycled composites can be explained on the basis of emission and punching out of dislocations from the interfacial region [99]. The plastic strain of Al/SiC_p composite was observed to be increasing when compared with unreinforced aluminium due to CTE mismatch between the aluminium matrix and SiC particles during thermal cycling [16].

The thermal stresses generated in SiC_p reinforced aluminium matrix during the early stages of thermal cycling relaxes by creep at temperatures above 90°C. Development of strain hysteresis loops and residual plastic strains were observed in Al-Mg alloy reinforced with fly

ash during thermal cycling. Further addition of fly ash resulted in the reduction of residual plastic strains thereby increasing the dimensional stability of the composite [100,101]. Co-continuous composites such as NiAl-Al₂O₃ and Al-Al₂O₃ show more resistance to thermal cycling damage when compared with traditional composites [102].

Investigations on the thermal cycling behaviour of ultra high modulus carbon fibre reinforced aluminium alloy matrix composite revealed occurrence of microcracks and debonding at the interface region which increased with the temperature difference. Bending modulus of the composite showed an abrupt increase initially and then decreased with thermal cycles due to generation and propagation of microcracks. The amount and length of pull-out fibre was seen to be increasing with the number of cycles irrespective of temperature difference. Even though there is a gradual increase in dislocation density in the Al matrix with the number of thermal cycles; it will eventually decrease after a certain period due to the movement and annihilation of dislocations of opposite sign [103]. Thermal cycling tests conducted on a saffil fibre reinforced 2014 aluminium alloy matrix resulted in an interfacial reaction which strengthened the composite and led to a decrease in its coefficient of thermal expansion [104]. Thermal–mechanical cycling (TMC) could induce interfacial degradation in the case of boron fibre-reinforced aluminium matrix composite. This effect increases with the number of TMC cycles and the applied stress levels [105].

6. Thermal Expansion

Low and stable coefficient of thermal expansion (CTE) is a necessity for components which are subjected to a change in temperature such as structural parts in aerospace, automobiles, sensors, measuring instruments, microwave components etc [106]. Due to suitability of AMCs for elevated temperature applications, studying their thermal expansion property is of considerable practical interest. The coefficient of thermal expansion (CTE) of MMCs can be tailored by controlling the reinforcement type, size, morphology and relative quantity [107-

110]. The thermal expansion behaviour of metal matrix composites, especially AMC is very complicated since the metal matrix can deform plastically in reaction to the thermal stresses generated. Super plastic flow behaviour exhibited by metal matrix composites during thermal cycling is due to the generation of internal stresses which results from the difference in thermal expansion coefficient the matrix and the reinforcement [111-113]. Plastic deformation will get increased at elevated temperatures as thermal strains are a function of the temperature which increases with temperature [114]. Internal stresses generated due to the CTE mismatch between fibres and matrix strongly affect the thermal expansion behaviour and dimensional stability of aluminium matrix composites [115].

In the case of particulate reinforced aluminium matrix composites it was observed that the CTE of the composite can be reduced substantially by the addition of reinforcement particles to the aluminium matrix [116,117]. Also the CTEs of both the composite and the unreinforced Al matrix were found to be increasing with temperature. The restriction imposed by the particles on the Al matrix during thermal expansion resulted in slower increasing rate of CTE of composite, compared to that of unreinforced Al [118]. In the case of SiC coated boron fibre reinforced aluminium matrix composites fabricated by hot pressing the thermal expansion measured perpendicular to the fibres was found to be in good agreement with that predicted by theoretical models whereas thermal expansion measured in the fibre axis direction was lower than that of theoretical predictions due to the yielding in the matrix [119]. Anisotropy of fibre thermal expansion observed in the case of graphite fibre can eliminate yielding of the matrix due to thermal stress [27]. Experimental measurement of the thermal expansion behaviour of both unreinforced 2080 Al and Al/SiC_p extruded composites revealed that anisotropic distribution of SiC particles decides the anisotropic thermal behaviour of Al/SiC_p composites. Also both the particle volume fraction and the orientation relative to the extrusion direction have prominent effect on the CTE of composite. The FEM

results used to simulate the thermal behaviour showed that orientation of SiC particles changes the internal stress in the composite, which results in anisotropic thermal behaviour [120].

Thermal deformation measurement in aluminium matrix composites can be performed using a non-destructive optical technique known as Digital speckle pattern interferometry (DSPI) without any restriction on the shape of the specimen [121]. Increasing volume fraction of saffil fibres caused a decrease in the value of coefficient of thermal expansion of aluminium matrix composite. An elastic response at lower temperatures and a plastic response at higher temperatures were exhibited by the measured CTE of the composite [122]. A semi-empirical method for determining the average coefficient of thermal expansion (CTE) of components in an Al-SiC composite system depicted that when the volume fraction of SiC was increased, the average volumetric CTE of both the fibre and the matrix were observed to be decreasing [123-125]. The incorporation of alumina fibres as reinforcement into Zn-Al alloys results in a significant reduction in the creep rate and the coefficient of thermal expansion [126]. Out of the aluminium matrix composites prepared using the reinforcements such as carbon, SiC, Al₂O₃ and boron fibres, anisotropy of the CTE was found to be very large for aluminium matrix composites reinforced with carbon fibres [2]. SiC_p reinforced Al alloy composite fabricated by stir casting exhibited lower coefficient of thermal expansion values than the Al alloy [127].

A monotonic increase in CTE with plastic prestrain was observed in alumina particle reinforced aluminium matrix composites over smaller temperature ranges. But CTE increase was greater for the composite with higher volume fraction of alumina particles when they are studied over a wider temperature change. Also, particle cracking in particle reinforced MMCs can be monitored using CTE measurements [128]. Plastic yielding and flow of matrix void nucleation and volume fraction of broken particles have a prominent influence on the CTE of

the composite [15]. In the case of SiC particle reinforced aluminium matrix composites produced by vacuum assisted high pressure infiltration, the CTE of the composite increased with the size of the particles [129]. The effect of phase connectivity (i.e. metal-matrix, ceramic-matrix and interpenetrating where both phases form a continuous network in space) has a strong influence on the thermal expansion behaviour of SiC/Al system with the metal-matrix and ceramic-matrix cases showing the highest and lowest CTE values, respectively [130]. The damping capacity of aluminium matrix composites increases with the increase in temperature whereas the dynamic modulus was found to decrease with the increase in temperature. The Dislocations induced in the matrix alloy due to coefficient of thermal expansion (CTE) mismatch between the constituent phases explains the damping capacity of the AMCs at low temperatures, whereas matrix–reinforcement interface and thermo elastic damping explains the damping capacity at higher temperatures [131].

The CTE curves can be used to qualitatively predict the thermal mismatch stress (TMS) and change of its states, as observed in the case of a SiC whisker reinforced aluminium matrix composite, where the CTE of the composite was fluctuating with test temperature due to the presence of larger elastic and plastic thermal mismatch stress in the matrix. Within most temperature ranges, the natural shrinkage of the matrix was observed to keep a balance with the plastic relaxation of the TMS in the matrix. The orientation distribution of SiC whiskers also influences the CTE of aluminium matrix composite [110,132-135]. The CTE of the aluminium matrix composite containing β -eucryptite particles and aluminium borate whiskers fabricated by squeeze casting technique was affected significantly by the degree of interfacial reaction on the surface of β -eucryptite particle. Stronger interface between the β -eucryptite particle and the Al matrix resulted in lower CTE of the composite [105,136,137]. The overall CTE of aluminium matrix composite is mainly determined by the total volume fraction of the reinforcement than the average particle size and particle size distribution [138,139]. The

coefficients of thermal expansion of SiC_p/Al composite and unreinforced Al matrix fabricated by squeeze casting method displayed maxima at 250°C and 350°C, respectively, as shown in Fig.5 which then got reduced at higher temperatures. The increase in solubility of Si in Al due to the increase in temperature is mainly responsible for this behaviour. Hence, the thermal expansion behaviour is greatly influenced by the heterogeneities of Al-based materials [140-142]. The temperature dependence of the solubility of Si in Al also influences the CTE of Al–Si matrix alloys significantly. In the case of SiC particulate reinforced aluminium-matrix composites it was observed that visco-plastic matrix deformations and changing void volume fractions were responsible for the anomalies in CTE of the composite [143]. Thermal-mechanical cycling significantly affect the thermal expansion behaviour of boron fibre-reinforced aluminium matrix composite by inducing interfacial degradation, which increases with the number of cycles. Thermal expansion behaviour of the composite would depend on the thermal expansion of the fibres, when there is no interfacial sliding or fibre fracture observed during CTE measurement [104].

Hybrid Al composites reinforced with SiC foam and SiC particles developed using squeeze casting technology displayed lower CTE values than those of SiC particle reinforced aluminium composite with same SiC content. This was attributed to the characteristic interpenetrating structure of hybrid composite which makes them suitable to be used as an electronic packaging substrate material [144]. The strengthening due to CTE mismatch was not observed in the case of a bulk particulate reinforced nanostructured aluminium matrix composite which was fabricated by cryomilling and subsequent consolidation, since the formation of geometrically necessary dislocations was constrained to a nanostructured interfacial region containing grains 30-50nm in size [145]. The coefficient of thermal expansion of aluminium–graphite composites fabricated by vacuum hot pressing was

observed to be decreasing with increasing flake graphite. A control in CTE of the composite was achieved by controlling the graphite percentage [146].

Phase transformation of reinforcement particle can also affect the thermal expansion behaviour of aluminium matrix composite. In the case of β -eucryptic particle reinforced aluminium matrix composites prepared by spark plasma sintering, it was observed that the metastable phase of eucryptic particle got transferred to normal eucryptic phase due to stress relaxation by annealing process. This transformation of the metastable phase has a prominent effect on the thermal expansion behaviour of the composite [147,148].

Thermal expansion behaviour of carbon fibre reinforced Al composite is mainly determined by the thermal expansion of aluminium matrix and the restriction of carbon fibre through interfaces. This signifies the importance of interface on the thermal expansion behaviour of composite [149]. The coefficient of thermal expansion (CTE) has close relationship with the changing rate of thermal mismatch stress and the dislocation density of matrix. This was observed in the case of SiC whisker reinforced aluminium composite where the composites were cooled down from 580°C with lower and higher cooling rates. Analysis pointed out that the dislocation density and thermal mismatch stress (TMS) was lower in slowly cooled composite compared to fast cooled (water quenched) composite. Hence cooling rate greatly influences the thermal expansion behaviour of aluminium matrix composites [9].

The thermal expansion response of the fibre-reinforced composites differ from that of the particulate composites as they show only very small residual strains when they are cooled down from the peak temperature to room temperature [113]. When the fibre content of continuous Mo fibre reinforced AMCs produced by diffusion bonding was increased, the CTE of the composites decreased as close to the values of Mo fibres. Moreover, the CTE of the unidirectional composite was found to be increasing with increase in temperature,

whereas in the case of dual directional composites, with increasing temperature the CTE first decreased due to the expansion constraints created by large accumulated thermal stress, then after reaching a minimum at about 250°C, it starts increasing which may be attributed to matrix yielding and interfacial decohesion [1].

Multi-walled carbon nanotubes reinforced aluminium matrix composites are promising material for space structures and electronic packaging due to their low CTE value [150,151]. Recently, Lei et al. [152] studied the thermal expansion behaviour of aluminium matrix composites reinforced with hybrid (nanometer and micrometer) alumina particles and observed that nanoparticle concentration had an important effect on the CTE of the composite. Stress relaxation process determines the CTE of composites with lower nanoparticle concentration whereas percolation process determines the CTE of composites with higher nanoparticle concentration.

7. Thermal Fatigue

Thermal fatigue is caused mainly due to the cyclic change of temperature and complete or partial restriction of thermal deformation due to external or internal limitations which can lead to fatigue cracking at locations with stress concentration. The study of thermal fatigue behaviour of particulate reinforced aluminium matrix composites are of great importance since they are frequently used in components of engineering applications such as connecting rods and cylinder liners that may undergo thermal fatigue during service due to internal and external restriction against thermal expansion and contraction [153,154]. It is one of the foremost design considerations in diesel engines [155].

Generally the fatigue behaviour of discontinuously reinforced metal matrix composites is characterized by the competition between the cyclic hardening process and the cyclic softening process which occurs at elevated temperature. Formation of new dislocations in the

matrix and interaction among them constitutes the cyclic hardening behaviour whereas interface failure, matrix cavitation, precipitate coarsening and the rearrangement and annihilation of dislocations constitutes the cyclic softening process [154]. The dependence of fatigue behaviour on temperature and particle size at elevated temperatures are mainly attributed to the cyclic softening taking place which results in reduction of strength in the matrix [156]. Combinations of cyclic hardening and cyclic softening to failure were observed in aluminium alloy matrix discontinuously reinforced with SiC particles during fully-reversed strain amplitude control [157-159].

Cyclic softening was observed in an alumina reinforced 6061-T6 aluminium alloy composite at lower strain amplitudes, independent of test temperature. At high strain amplitude, the composite displayed cyclic hardening. Also, the low cycle fatigue behaviour of composite was inferior to that of the unreinforced 6061-T6 Al alloy, especially in the short-life, high-amplitude region. The cyclic yield stress decreased with the test temperature. In the high cycle fatigue region, the fatigue lives are generally controlled by strength [8]. Submicron-scale alumina particle reinforced aluminium alloy fabricated using powder metallurgy displayed cyclic hardening behaviour under tension and cyclic softening behaviour under compression at small strain amplitudes during low-cycle fatigue testing. Rapid stabilization of cyclic deformation was observed in the composite which produced symmetric stress-strain hysteresis loops at higher strain amplitudes. Bauschinger effect was observed at small strain amplitudes due to constrained cyclic deformation created by the distribution of particle clusters [160].

The main thermal fatigue fracture mechanisms operating in aluminium matrix composites are interfacial decoherence between particle and matrix, particle breakage and crack propagation. Fatigue crack initiation was always generated in the inclusion or particle cluster area [8,161-163]. Particle breakage was rare at higher temperatures and most of the cracks were nucleated

in the matrix [154,164,165]. In the fatigue behaviour study of aluminium matrix composites reinforced with SiC particles, thin matrix ligaments which separate the uncracked subsurface particles from free specimen surface were found to be the fatigue crack initiation sites for specimens with smaller size SiC particles. But, for specimens with larger size SiC particles, crack initiation occurred within the particle [166]. Thermal fatigue damage induced in SiC particulate reinforced 6061 Al composite as a result of repeated pulsed laser heating and mechanical load was studied and it was found that the damage was initiated at the intersection region of laser irradiated brim region and the perpendicular direction of tensile load [167].

The crack initiation of SiC particulate reinforced aluminium alloy composite subjected to fully reversed axial fatigue tests, was found to be dependent on temperature and particle size [156]. In the numerical investigation made on alumina reinforced aluminium matrix composite under low cycle fatigue it was found that stress and strain concentrations in the microstructure plays a major role in the formation of extrusions and intrusions which subsequently leads to fatigue crack initiation [168]. Particle fracture, debonding and matrix cracking were the chief damage mechanisms that causes fatigue damage in alumina particulate reinforced 6061 Al matrix composite. Short fatigue crack initiation and extension can occur due to damage localization caused by lump of alumina reinforcement particles. The hysteresis loop variation of strain-controlled cylindrical specimens subjected to low cycle fatigue test pointed out cyclic plastic strain as the suitable low cycle fatigue damage parameter [169].

The fatigue crack propagation in aluminium matrix composites takes place preferentially through the matrix region. Decrease in the micro-hardness value of composite promotes increased crack propagation speed [170]. Higher fatigue life and tensile strength were observed for 2124 aluminium alloy reinforced with SiC particles when compared with the

unreinforced Al alloy. By decreasing SiC particle size and increasing SiC volume fraction, the strength and fatigue life of the composite was found to be increasing. Size and volume fraction of SiC particles, stress intensity maximum at crack tip and the matrix strength governs the frequency of particle fracture during fatigue crack propagation [171]. The cyclic plastic deformation taking place in the fatigue-damaged zone is considered to be the main mechanical driving force for the fatigue crack growth [172,173]. The retardation of fatigue crack growth was observed when crack propagated from low-high volume fraction of SiC and the deflection of cracks also decreased the crack growth rate [174,175].

The thermal fatigue crack initiation and propagation in SiC_p/Al composite fabricated by infiltration technique takes place mainly by fracturing of the large reinforcing particles in the composite by thermal shock. SEM micrographs representing the initiation and propagation of thermal fatigue crack in Al matrix containing 65vol% SiC and 35vol% SiC are shown in Fig.6 below. Also it was observed that by reducing the size of the reinforcing particles, the thermal fatigue resistance of the composite was found to be increased [153].

Debonding and cracking of the interface were the main degradation mechanisms associated with the zero load thermal fatigue testing of aluminium matrix composites with weak interface; whereas matrix plastic deformation and interfacial product formation were the degradation mechanisms associated with that of strong interface. All these degradation mechanisms are attributed to the CTE mismatch between the fibre and the Al matrix. [176-178]. Powder metallurgy processing was used to fabricate aluminium matrix composite with nickel-titanium (Ni-Ti) shape memory alloy as the reinforcement phase. On comparison with the unreinforced Al, the fatigue life, yield strength and ultimate strength of the composite was found to be enhanced due to the strengthening effect produced as a result of shape memory effect exhibited by the Ni-Ti alloy. Due to shape memory effect, residual internal stresses were created around each particle which resulted in the strengthening of the composite [179].

Cyclic softening was observed in SiC whisker reinforced 6061Al matrix composites during out-of-phase (OP) and in-phase (IP) thermo-mechanical fatigue (TMF) tests. Thermal and mechanical cyclic strains are applied simultaneously to the material during these tests. Also, compressive mean stress and tensile mean stress were generated during IP and OP-TMF, respectively [180]. In the case of thermal fatigue tests conducted on the aluminium alloy EN AW-6061-T6 reinforced with Al₂O₃ particles fabricated using stir casting, more damage was observed near to the particles due to thermal and mechanical mismatch of the phases. Four mechanisms causing damage and residual stress development were reported which includes: thermally induced global deformation due to inhomogeneous distribution of temperature, thermally induced local deformation due to coefficient of thermal expansion (CTE) mismatch, mechanically induced local deformation due to different deformation behaviour of both phases and overaging. Global deformation was the dominant mechanism in non-reinforced alloy whereas in composite, local mechanisms were significant [181]. Thermal fatigue of short fibre reinforced aluminium AE42 alloys was investigated with an emphasis on the changes in the strain and hardness before and after thermal cycling. It was observed that the thermal strain was affected by experimental condition of the thermal cycling and the strength of matrix. After thermal cycling, a decrease in hardness was observed due to the occurrence of matrix overaging and recovery [182,183].

8. Thermal Conductivity

One of the major advantages offered by the metal matrix composites is that by suitably selecting the reinforcement phase and matrix variables, thermal properties of the composite can be tailored in such a way as to make it appropriate for electronic packaging applications. Particularly, there should be a proper matching between of CTE of materials used for heat dissipation with that of semi-conductors and ceramic insulators in electronic packaging so as to prevent solder-joint failure during thermal cycling [184,185]. For example, the heat

generated due to high power densities of power electronic devices such as IGBT (Insulated Gate Bipolar Transistor) should be transported from the ceramic chips to the ceramic substrate and then through the solder and the base plate into a heat sink. Here if there is no proper matching of CTE between the components then it may lead to delamination of the solder when there is a change in temperature [186]. The CTE of metals can be lowered can be lowered by reinforcing them with low CTE fillers. Ceramics such as SiC and AlN are suitable for this purpose as they have both high thermal conductivity and low CTE.

The study of thermal conductivity of AMCs is important since they are increasingly considered as a promising material for thermal management applications. Al has high thermal conductivity and also high value of CTE. For lowering the CTE of Al it has to be reinforced with a higher volume fraction of filler material. Liquid metal infiltration is thus a suitable fabrication process for AMCs since it allows high reinforcement volume fractions (upto 70%) in addition to its near net shape producing capability. AMCs with high volume fractions of SiC, AlN etc are used in a number of electronic applications. Increasing volume fraction of these ceramic reinforcements in Al matrix also increases its brittleness which is acceptable for electronic applications. In addition to liquid metal infiltration, other liquid phase techniques such as stir casting and compo casting can also be used for the fabrication of AMCs with high volume fraction of reinforcements. Using powder metallurgy route, fabrication of AMCs with high reinforcement volume fractions is difficult since the formation of protective alumina layer on surface of each Al particle hinders the sintering process. The thermal conductivity of composites relies on a variety of parameters which includes the thermal conductivity of the constituent phases, their volume fraction and shape, and also the size of the inclusions due to a finite metal/ceramic interface thermal resistance [184,187-189].

By examining the literature it has been observed that the most common ceramic particle used for reinforcing Al matrix is silicon carbide (SiC) because of its low cost and low CTE

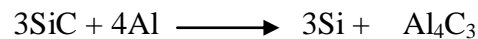
[184,186]. A low value of thermal conductivity was observed in the SiC particulate reinforced aluminium matrix composite produced by plasma spraying of the ball milled pure Al powders with 55 and 75 vol% SiC particles. Thermal boundary resistance offered by the interfacial gaps formed at the Al/SiC interface was found to be the dominant factor responsible for lowering the value of thermal conductivity. Porosity, Iron impurity, longer ball milling time and finer SiC size also lowers the thermal conductivity of the composite. Hot rolling and hot isostatic pressing treatment can be performed to improve the thermal conductivity as it improve the interfacial bonding and porosity of the composites. The decline in thermal conductivity value due to the finer SiC particle size is due to the fact that as particle size becomes small, there will be a large contribution of interface to thermal resistance [187,190].

The effect of SiC particle size distribution on thermal conductivity of Al matrix composite was studied by Molina et al. [191] where monomodal and bimodal size distributions of SiC particles were compared. In the case of composite based on powders with monomodal size distribution, a steady increase in thermal conductivity was observed. For bimodal particle mixtures thermal conductivity started increasing with increasing volume fraction of coarse particles and then reached a roughly constant value. A theoretical model based on equivalent diameter approach (EDA) was successful in predicting whether the composite system such as Al/SiC_p with multimodal particle mixtures can acquire an appropriate distribution design for attaining better thermal conduction properties [192].

In the case of SiC_p/Al composites with high particle volume fraction fabricated by spark plasma sintering [193], a small portion of pores can always appear as an unavoidable phase because of the non-wetting nature of SiC and aluminium, resulting in weak interfaces and incomplete sintering. The effect of porosity on the thermal conductivity of SiC particulate reinforced aluminium matrix composite was analysed numerically using a model based on the

effective medium approximation (EMA) scheme. Porosity can intensely deteriorate the thermal conductivity of the composite by scattering the flow of heat. EMA approach was found to be in good agreement with the experimental data, especially with porosity below 10%, but for higher levels, predictions were a bit higher compared to the experimental values. Furthermore, microstructural features such as voids and matrix/particle interface status also contribute to decrease in thermal conductivity as they scatter the heat flow around them [194].

Bad wettability and formation of undesirable interfacial brittle reaction product (Al_4C_3) are the main problems faced with the processing of SiC particulate reinforced aluminium composites. Aluminium carbide (Al_4C_3) weakens the interface and by reacting with atmosphere moisture degrades thermal properties.



The Si which is the other reaction product forms also creates non-uniformity in phase distribution and mechanical property distribution by dissolving in the aluminium matrix and substantially lowering its melting point. The wettability of SiC_p/Al composites can be enhanced by the co-addition of Si and Mg to it, but care must be taken to maintain a balance between the wettability improvement and prevention of interfacial reaction for obtaining optimum properties. Using Al-Si alloy as the matrix is one of the effective way to reduce the interfacial reaction as the Si present in the alloy promotes an opposite reaction to that of interfacial reaction and suppresses it. But the disadvantage is that since Al-Si alloy is less ductile compared to aluminium matrix, it will decrease the mechanical properties of the composite [184, 188]. The thermal conductivity of SiC particle reinforced Al matrix composite decreased with increasing the amount of SiC and increased with increasing SiC particle size [195].

Aluminium nitride reinforced aluminium matrix composites offers better thermal conductivity than SiC/Al composites due to non-reactivity of AlN with aluminium. Thermal conductivity of aluminium nitride particle reinforced composites is very sensitive to the relative packing density of the composite [184,196,197].

Alumina also does not react with aluminium but its agglomeration tendency and low value of thermal conductivity limits its usage [184]. Thermal conductivity was found to vary linearly with temperature in the case of Al/Al₂O₃-MMC prepared by powder metallurgy method. Also the thermal conductivity of composites decreases with increasing Al₂O₃ volume fraction and decreasing Al₂O₃ particle size [198]. Thermal conductivity of Al₂O₃ reinforced Al-AlN matrix composite showed a marginal decrease with increase in temperature upto 150°C. Carbon fibres, carbon nanotubes and diamond particles are also used as filler material for aluminium matrix composites in a number of studies [13,185,199-213].

Mizuuchi et al. [214] measured the thermal conductivity in diamond particle dispersed aluminium matrix composites which were fabricated in solid-liquid coexistent state from the powder mixture of diamond, pure Al and 5056-type Al-Mg alloy by spark plasma sintering (SPS) process. The thermal conductivity of the Al matrix composite containing 45.5 vol % diamond reached 403 W/mK, approximately 76% the theoretical thermal conductivity estimated by Maxwell-Eucken's equation. No interfacial reaction was observed between the diamond particle and the Al matrix.

A steady increase of thermal conductivity was observed in aluminium matrix composites reinforced with mixtures of diamond and SiC particles of equal size which were fabricated by gas pressure-assisted liquid metal infiltration. Replacing SiC gradually by diamond particles results in this increase and thermal conductivity of the nominally pure aluminium matrix is influenced by take-up of some silicon from the silicon carbide [215]. Vacuum hot pressing is

better than spark plasma sintering to fabricate diamond/Al composites with high thermal conductivity for heat management applications [216]. Also the contact time between melt and diamond reinforcement during liquid infiltration processing and the addition of silicon to the Al matrix material were found to significantly affect the thermal conductivity of the composites by modification of the interface [185].

9. Conclusions

Detailed review was carried out on the behaviour of aluminium matrix composites under different kinds of thermal stresses and the following conclusions were made:

- i. Residual thermal stresses generated in AMCs increases with increasing volume fraction of the reinforcement and decreases with increase in interparticle spacing. They improve the hardness and strength when the AMC is cooled from low fabrication temperature. But when the composite is cooled from high fabrication temperature, residual stress relaxation mechanisms become prominent and plastic deformation takes place which results in premature yielding prior to loading. The magnitude of the thermal stress also increases with the increase in processing temperature.
- ii. The internal stresses generated which either block or assist the motion of individual dislocations determines the thermal cycling behaviour of AMCs. Strength, damping capacity and dimensional stability of AMCs are improved by thermal cycling treatment when the internal stresses generated due to them blocks the dislocation movement. On the other hand, thermal stresses produced by thermal cycling can increase the plasticity at the interface resulting in plastic deformation at stresses lower than their yield stress. In combination with relatively small applied loads thermal cycling can result in superplastic deformation of the composite to very large strains (> 300%).

- iii. The coefficient of thermal expansion of AMCs can be lowered by increasing the volume fraction of the reinforcement and decreasing the particle size. CTE of composite is mainly determined by the thermal expansion and heterogeneities of the aluminium matrix.
- iv. The thermal fatigue resistance of AMC can be increased by increasing the reinforcement volume fraction and decreasing the particle size. During elevated temperatures, cyclic softening was observed at low strain amplitudes and cyclic hardening was prominent at high strain amplitudes. Fatigue crack initiation always occurred in the inclusion or particle cluster area and the fatigue fracture mechanisms were crack propagation, particle breakage and interfacial decoherence between the particle and the matrix.
- v. The thermal conductivity of AMCs decreased with increase in reinforcement volume fraction. The reduction in particle size also lead to decrease in thermal conductivity due to the large contribution of interfacial thermal resistance. Presence of pores and voids scatter heat flow and severely lowered the thermal conductivity of the AMCs.

10. Future research scope

Tailoring the interfacial thermal mismatch and multiplying or reducing the thermal stresses of aluminium matrix composites for achieving desired properties is an area facing dearth in literature. Proper understanding of mechanism of thermal conductance is required for meeting the ever-growing demands of electronics industry. Thermal history of advanced metal matrix composites with hybrid reinforcement distribution also lacks detailed study.

Acknowledgement

The authors would like to acknowledge the National Institute of Technology (NIT), Rourkela for providing the necessary financial and infrastructural support.

References

- [1] Chen LG, Lin SJ, Chang SY. *Compos. Sci .Tech* 2006, 66, 1793-1802.
- [2] Mykura H, Mykura N. *Compos. Sci .Tech* 1992, 45,307-312.
- [3] Tan MJ, Chew MC, Hung NP, Sano T. *J. Mater. Process. Tech* 1997, 67, 62-66.
- [4] Degischer HP, Prader P, Marchi, CS. *Composites Part A* 2001, 32, 1161-1166.
- [5] Surappa MK. *Sadhana-Acad P Eng S* 2003, 28,319-334.
- [6] Cayron C <http://cimewww.epfl.ch/people/cayron/Fichiers/thesebook-chap1.pdf>
Accessed 23 July 2013.
- [7] <http://libback.uqu.edu.sa/hipres/Indu/indu10542.pdf> Accessed 23 july 2013.
- [8] Perng CC, Hwang JR, Doong JL. *J Compos. Sci .Tech.*1993, 49,225-236.
- [9] Fei WD, Hu M,Yao CK. *Mater. Chem. Phys.*2002, 77,882-888.
- [10] Chen YC, Daehn GS, Wagoner RH. *Scripta Metall Mater.*1990, 24, 2157-2162.
- [11] Tjong SC, Tam KF, Wu SQ. *Compos. Sci .Tech.* 2003, 63, 89-97.
- [12] Sayman O,Ozer MR. *Compos. Sci .Tech.* 2001, 61, 2129-2137.
- [13] Mizuuchi K, Inoue K, Agari Y, Morisada Y, Sugioka M, Tanaka M, Takeuchi T,
Kawahara M, Makino Y. *Composites: Part B.* 2011,42,1029-1032.
- [14] Ozdemir I, Onel K. *Composites: Part B.*2004, 35,379-384.

- [15] Nam TH, Requena G, Degischer P. *Composites: Part A* 2008, 39, 856–865.
- [16] Chen N, Zhang H, Gu M, Jin Y. *J Mater Process Tech* 2009,209,1471-1476.
- [17] Rao VV, Murthy MVK, Nagaraju J. *J. Compos. Sci .Tech* 2004, 64, 2459–2462.
- [18] Rosso M. *J Mater Process Tech* 2006,175, 364–375.
- [19] Chawla KK, Chawla N.<http://enpub.fulton.asu.edu/chawla/papers/Wileymmcfinal.pdf>
 Accessed 3 December 2013.
- [20] Agrawal P, Conlon K, Bowman KJ, Sun CT, Cichocki FR, Trumble KP. *Acta Materialia* 2003, 51, 1143–1156.
- [21] Shieu FS, Raj R, Sass SL. *Acta metal, mater.*1990, 38, 2215-2224.
- [22] Ho S, Saigal A. *Acta metall, mater.* 1994,42,3253-3262.
- [23] Douina J, Donnadieub P, Finela A, Dirrasc GF, Silvaind JF. *Composites: Part A* 2002, 33, 1397-1401.
- [24] Daehn GS, Hebbar K, Suh YS, Zhang H. *Compos Eng* 1993, 3, 699-713.
- [25] Tsai SD, Mahulikar D, Marcus HL. *Mater Sci Eng*, 1981, 47,145 – 149.
- [26] Shorshorov MKH, Ustinov LM, Kuznetsov YUG, Vinogradov LV, Jamnova VI. *Composites* January 1976.
- [27] Vedula M, Pangborn RN, Queeney RA. *Composites* 1988,19,1.
- [28] Tang T, Horstemeyer MF, Wang P. *Int J Eng Sci* 2012, 51,161-167.
- [29] Sayman O. *Composites: Part B* 2005, 36, 61-72.
- [30] Zywicz E, Parks DM. *J. Compos. Sci .Tech* 1988, 33,295-315.

- [31] Vedula M, Pangborn RN, Queeney RA. *Composites* 1988,19,2.
- [32] Liu HT, Sun LZ. *Int J Solids Struct* 2004, 41, 2189-2203.
- [33] Arsenault RJ, Taya M. *Acta metall* 1987, 35,651-659.
- [34] Withers PJ, Stobbs WM, Pedersen OB. *Acta metall* 1989, 37, 3061-3084.
- [35] Lilholt H. *Mater Sci Eng A* 1991, 135,161-171.
- [36] Povirk GL, Needleman A, Nutt SR. *Mater Sci Eng A* 1990,125,129-140.
- [37] Povirk GL, Needleman A, Nutt SR. *Mater Sci Eng A* 1991,132,31-38.
- [38] Li DS, Wisnom MR, Dingley DJ. *Compos. Sci .Tech* 1991, 42,413—427.
- [39] Jiang Z, Li G, Lian J, Ding X, Sun J. *Compos. Sci .Tech* 2004, 64, 1661-1670.
- [40] Meijer G, Ellyin F, Xia Z. *Composites: Part B* 2000, 31, 29–37.
- [41] I. Dutta. *Compos. Sci .Tech* 1991, 41,193-213.
- [42] Sajjadi SA, Ezatpour HR, Parizi MT. *Mater Design* 2012, 34,106–111.
- [43] Allen AJ, Bourkei AM, Dawesi S, Hutchings T, Withers PJ. *Acta metal mater.* 1991,40,2361-2372.
- [44] Fitzpatrick ME, Withers PJ, Baczmanski A, Hutchings MT, Levy R, Ceretti M, Lodini A. *Acta mater* 2002,50,1031–1040.
- [45] Schobel M, Altendorfer W, Degischer HP, Vaucher S, Buslaps T, Michiel MD, Hofmann M. *Compos. Sci .Tech* 2011, 71,724–733.
- [46] Shee SK, Pradhan SK, De M. *Mater Chem Phys* 1998, 52,228-234.
- [47] Nakamura T, Suresh S. *Acta metall mater* 1993, 41, 1665-1681.
- [48] Dutta I, Sims JD, Seigenthaler DM. *Acta metall mater* 1993, 41,885-908.
- [49] Ho S, Saigal A. *Acta metal mater.* 1994, 42, 3253-3262.
- [50] Ho S, Saigal A. *Mater Sci Eng A* 1994, 183, 39-47.

- [51] Jeong GS, Allen DH, Lagoudas DC. *J Solids Structures* 1994, 31, 2653-2677.
- [52] Gupta N, Nguyenb NQ, Rohatgi PK. *Composites: Part B* 2011, 42,916–925.
- [53] Xuea J, Wangb WX, Takao Y, Matsubara T. *Composites: Part A* 2011, 42,986–992.
- [54] Hanus E, Ericsson T. *Mater Sci Eng A* 1995, 90,155-163.
- [55] Lee RS, Chen GA, Hwang BH. *Composites* 1995, 26,425-429.
- [56] Singh SB, Ray S. *J Mater Process Tech* 2003, 143–144,623–628.
- [57] Altan G, Topcu M, Bektas NB, Altan BD. *J Mech Eng Sci*, 22, 2318-2327.
- [58] Bouafia F, Serier B, Abbas B, Bouiadjra B. *Comp Mater Sci* 2012,54,195–203.
- [59] Guagliano M. *J Mater Eng Perform* 1998, 7,183-189.
- [60] Morelli1 EC, Urreta SE, Schaller R. *Acta mater* 2000, 48, 4725–4733.
- [61] Wu PL, Tian Z, Wang LD, Fei WD. *Thermochim Acta* 2007,455,7–10.
- [62] Furness JAG, Clyne TW. *Mater Sci Eng A* 1991,141,199-207
- [63] Daehn GS, Hebbbar K, Suh YS, Zhang H. *Compos Eng* 1993, 3,699-713.
- [64] Flour JCL, Locicero R. *Scripta Metall Mater* 1987, 21, 1071-1076.
- [65] Zhang H, Daehn GS, Wagoner RH. *Scripta Metall Mater*. 1990,24,2151-2155.
- [66] Chen YC, Daehn GS. *Scripta Metall Mater* 1991, 25, 1543-1548.
- [67] Sherby OD, Wadsworth J. *Prog Mater Sci* 1989,33,169-221.
- [68] Hall IW, Patterson WG. *Scripta Metall Mater* 1991, 25, 805-810.
- [69] Pickardi SM, Derby B. *Acta metall mater*. 1991, 38, 2537-2552.
- [70] Cheong YM, Marcus HL. *Scripta Metall Mater* 1987, 21, 1529-1534.
- [71] Daehn GS, Oyama T. *Scripta Metall Mater* 1988, 22, 1097-1102.
- [72] Doncel GG, Karmarkar SD, Divecha AP, Sherby OD. *Compos. Sci .Tech* 1989, 35,105-120.
- [73] Daymond MR, Withers PJ. *Scrita Mater* 1996, 35, 1229-1234.
- [74] Daymond MR, Withers PJ. *Scrita Mater* 1996, 35,717-720.

- [75] Daymond MR, Withers PJ. *Appl Compos Mater* 1997, 4,375–393.
- [76] Hong SI, Gray GT, Vecchio KS. *Mater Sci Eng A* 1993, 171,181–189.
- [77] Girard C, Fougères R, Vincent A. *J Alloy Compd* 1994, 211/212,169-172.
- [78] Pickard SM, Derby B. *Mater Sci Eng A* 1991, 135,213-216.
- [79] Aria FR, Lichti T, Gagnon G. *Scripta Metall Mater* 1993, 28,587.
- [80] Dunn ML, Taya M. *Mater Sci Eng A* 1994, 176,349-355.
- [81] Pal S, Bhanuprasad VV, Mitra R. *Mater Sci Eng A* 2008,489,11–20.
- [82] Colclough A, Dempster B, Favry Y, Valentin D. *Mater Sci Eng A* 1991, 135,203-207.
- [83] Ghorbel E. *Compos. Sci .Tech* 1997,57,1045-1056
- [84] Kehoe FP, Chadwick GA. *Mater Sci Eng A* 1991, 135,209-212.
- [85] Herr AE, Canumalla S, Pangborn RN. *Mater Sci Eng A* 1995, 200,181-191.
- [86] Wetland A, Johannesson T. *Mater Sci Eng A* 1995, 190,131-142.
- [87] Eggeler GF, Earthman JC. *Scripta Mater* 1998, 38,341-348.
- [88] Kuo SL, Kao PW. *Mater Chem phys* 1999, 58, 83-86.
- [89] Wu SQ, Wei ZS, Tjong SC. *Compos. Sci .Tech* 2000, 60, 2873-2880.
- [90] Dutta I. *Acta mater* 2000, 48, 1055-1074.
- [91] Badini C, Vecchia MLA, Giurcanu A, Wenhui J, *J Mater Sci* 1997,32,921–930.
- [92] Ozdemir I, Toparli M. *J Compos Mater* 2003, 37, 1839-1850.
- [93] Etter T, Papakyriacou M, Schulz P, Uggowitzer PJ. *Carbon* 2003, 41, 1017–1024.
- [94] Zhao M, Wu G, Zhu D, Jiang L, Dou Z. *Mater Lett* 2004, 58,1899–1902.
- [95] Chen AN, Arai Y, Tsuchida E. *Composites: Part B* 2005, 36,319–330.
- [96] Zhang H, Gu M. *J Alloy Comp* 2006, 426,247–252.
- [97] Huang YD, Hort N, Kainer KU. *Composites: Part A* 2004, 35,249–263.
- [98] Ozdemir I, Toparli M, Onel K, Tsunekawa Y. *J Compos Mater* 2005, 39,601-615.

- [99] Durieux S, Buffiere JY, Lormand G, Rapoport A, Vincent A. *Mater Sci Eng A* 1997,234,953-957.
- [100] Requena G, Yubero DC, Corrochano J, Repper J, GARces G. *Composites part A* 2012,43,1981-1988.
- [101] Uju WA, Oguocha INA. *Mater Sci Eng A* 2009, 526,100–105.
- [102] Rioja ED, Nasha JM, Williams JC, Breslin MC, Daehn GS. *Mater Sci Eng A* 2007, 463,115–121.
- [103] Daguanga L, Guoqin C, Longtao J, Ziyang X, Yunheb Z, Gaohui W. *Mater Sci Eng A* 2013,586,330–337.
- [104] Badinia C, Finoa P, Mussob M, Dinardo P. *Mater Chem Phys* 2000,64,247–255.
- [105] Qin YC, He SY, Yang DZ. *Mater Chem Phys* 2004, 86,204–209.
- [106] Fei WD, Wang LD. *Mater Chem Phys* 2004, 85,450–457.
- [107] Smagorinski ME, Tsantrizos PG, Grenier S, Cavašin A, Brzezinski T, Kim G. *Mater Sci Eng A* 1998,244,86–90.
- [108] Qing CG, Shu YW , Kang MA, Hussain M, Tao JL, Hui WUG. *Trans. Nonferrous Met. Soc. China* 2011, 21,262-273.
- [109] Zhiwu X, Jiuchun Y, Weiwei Z, Huibin X, Shiqin Y. *Compos Sci Tech* 2005,65,1461–1467.
- [110] Wang T, Fan T, Zhang D, Zhang G, Xiong D. *Mater Design* 2008,29,1275–1279.
- [111] Wu My, Sherby OD. *Scripta Metall Mater* 1984, 18,773-776.
- [112] Bohm HJ, Degischer HP, Lacom W, Qu J. *J. Compos Eng* 1995, 5, 37-49.
- [113] Kustov S, Golyandin S, Sapozhnikov K, Vincent A, Maire E, Lormand G. *Mater Sci Eng A* 2001,313, 218–226.
- [114] Vaidya RU, Chawla KK. *Compos Sci Tech* 1994, 50, 13-22.
- [115] Neite G, Mielke S. *Mater Sci Eng A* 1991, 148, 85-92.

- [116] Gudlur P, Forness A, Lentz A, Radovic M, Muliana A. *Mater Sci Eng A* 2012,531,18–27.
- [117] Uju WA, Oguocha INA. *Mater Des* 2012, 33,503–509.
- [118] Kima BG, Donga SL, Park S. *Mater Chem Phys* 2001, 72, 42–47.
- [119] Kreider KG, Patarini VM. *Metall Trans*, 1970, 1, 3431-3435.
- [120] Chawla N, Deng X, Schnell DRM. *Mater Sci Eng A* 2006, 426,314–322.
- [121] Aswendt P, Hofling R. *Composites* 1993, 24,611.
- [122] Kehoe FP, Chadwick GA. *Mater Sci Eng A* 1991, 135,209-212.
- [123] Lee YS, Gungor MN, Batt TJ, Liaw PK. *Mater Sci Eng A* 1991,145,37-46.
- [124] Chan KC, Liang J. *Compos Sci Tech* 2001, 61, 1265–1270.
- [125] Zhang Q, Wu G, Chen G, Jiang L, Luan B. *Composites: Part A* 2003, 34, 1023–1027.
- [126] Dellis MA, Keustermans JP, Delannay F. *Mater Sci Eng A* 1991, 135,253-257.
- [127] Karthikeyan B, Ramanathan S, Ramakrishnan V. *Mater Des* 2010,31,82–86.
- [128] Elomari S, Boukhili R, Lloyd DJ. *Acta mater* 1996, 44, 1873-1882.
- [129] Elomari S, Skibo MD, Sundarrajan A, Richards H. *Compos Sci Tech* 1998, 58,369-376.
- [130] Shen YL. *Mater Sci Eng A* 1998, 252,269–275.
- [131] Sastry S, Krishna M, Uchil J. *J Alloy Compd* 2001, 314,268–274.
- [132] Hu M, Fei WD, Yao CK. *Scripta Mater* 2002, 46,563–567.
- [133] Ohnuki T, Tomota Y. *Scripta Mater* 1996, 34,713-720.
- [134] Christman T, Suresh S. *Acta metal* 1988, 36, 1691-1704.
- [135] Qin CG, Yang XZ, Shu YW, Tao JL, Hui WUG. *Trans. Nonferrous Met. Soc. China* 2010, 20, 2143–2147.
- [136] Wang LD, Fei WD, Yao CK. *Mater Sci Eng A* 2002, 336,110–116.
- [137] Wang LD, Fei WD. *Mater Sci Eng A* 2006, 433,291-297.

- [138] Arpon R, Molina JM, Saravanan RA, Cordovill CG, Louis E, Narciso J. *Acta Mater* 2003,51,3145–3156.
- [139] Tjong SC, Tam KF. *Mater Chem Phys* 2006, 97, 91–97.
- [140] Zhang Q, Wu G, Jiang L, Chen G. *Mater Chem Phys* 2003,82,780–785.
- [141] Couturier R, Ducret D, Merle P, Disson JP, Joubert P. *J Eur Cem Soc* 1997,17,1861-1866.
- [142] Ejiogor JU, Reddy RG. *Mater Sci Eng A* 1999, 259,314–323.
- [143] Huber T, Degischer HP, Lefranc G, Schmitt T. *Compos Sci Tech* 2006, 66, 2206–2217.
- [144] Zhao LZ, Zhao MJ, Cao XM, Tian C, Hu WP, Zhang JS. *Compos Sci Tech* 2007, 67, 3404–3408.
- [145] Vogt R, Zhang Z, Li Y, Bonds M, Browning ND, Lavernia EJ, Schoenung JM. *Scripta Mater* 2009, 61, 1052–1055.
- [146] Chen JK, Huang IS. *Composites: Part B* 2013, 44,698–703.
- [147] Dong WL, Ye CUI, Tao YC, Peng WK, Dong FW. *Trans. Nonferrous Met. Soc. China* 2011, 21,280-284.
- [148] Wang LD, Xue ZW, Cui Y, Wang KP, Qiao YJ, Fei WD. *Compos Sci Tech* 2012,72,1613–1617.
- [149] He ZY, Hui WUG. *Trans. Nonferrous Met. Soc. China* 2010, 20, 2148–2151.
- [150] Deng CF, Ma YX, Zhang P, Zhang XX, Wang DZ. *Mater Lett* 2008,62,2301–2303.
- [151] Liu ZY, Xiao BL, Wang WG, Ma ZY. *Compos Sci Tech* 2012, 72, 1826–1833.
- [152] Lei Z, Zhao K, Wang Y, An L. *J Mater Sci Tech* 2013,
<http://dx.doi.org/10.1016/j.jmst.2013.04.022>.
- [153] Wu CML, Han GW. *Composites: Part A* 2006, 37, 1858–1862.
- [154] Llorca J. *Int J Fatigue* 2002, 24,233–240.

- [155] Song HW, Yua G, Tan JS, Zhou L, Yu XL. *Int J Heat Mass Tran* 2008, 51,757–767.
- [156] Uematsu Y, Tokaji K, Kawamura M. *Compos Sci Tech* 2008, 68, 2785–2791.
- [157] Srivatsan TS, Hajri MA. *Composites: Part B* 2002, 33,391–404.
- [158] Srivatsan TS, Hajri MA, Hannon W, Vasudevan VK. *Mater Sci Eng A* 2004, 379,181–196.
- [159] Zhang G, Li B, Zhang J, Cai W. *Prog nat sci* 2012,22,153-159.
- [160] Gasemn ZM, Ali SS. *Mater Sci Eng A* 2013, 562,109–117.
- [161] Akiniwa Y, Machiya S, Tanaka K. *Int J Fatigue* 2006, 28, 1406–1412.
- [162] Zhua SJ, Iizuka T. *Compos Sci Tech* 2003, 63,265–271.
- [163] Badinia C, Finoa P, Mussob M, Dinardo P. *Mater Chem Phys* 2000,64,247–255.
- [164] Tjong SC, Wang GS. *Mater Sci Eng A* 2004, 386, 48–53.
- [165] Tjong SC, Wang GS, Mai YW. *Compos Sci Tech* 2005, 65, 1537–1546.
- [166] Lukasak DA, Koss DA. *Composites* 1993,24,3.
- [167] Long SG, Zhou YC. *Compos Sci Tech* 2005, 65, 1391–1400.
- [168] Schneider Y, Soppa E, Kohler C, Mokso R, Roos E. *Proc Eng* 2011,10, 1515–1520.
- [169] Li C, Ellyin F. *Mater Sci Eng A* 1996, 214,115-121.
- [170] Wei Li, Zhenhua C, Ding C, Cang F, Canrang W. *J Alloy Compd* 2010,504,522–526.
- [171] Hall JD, Jones JW, Sachdev AK. *Mater Sci Eng A* 1994, 183, 69-80.
- [172] Ding HZ, Biermann H, Hartmann O. *Compos Sci Tech* 2002, 62, 2189–2199.
- [173] Ding HZ, Biermann H, Hartmann O. *Int J Fatigue* 2003, 25,209–220.
- [174] Xua FM, Zhua SJ, Zhao J, Qi M, Wang FG, Li SX, Wang ZG. *Mater Sci Eng A* 2003, 360,191-196.
- [175] Sharma MM, Ziemian CW, Eden TJ. *Mater Des* 2011, 32, 4304–4309.
- [176] Ghorbel E. *Compos Sci Tech* 1997, 57, 1045-1056.

- [177] Schoel M, Degischer HP, Vaucher S, Hofmann M, Cloetens P. *Acta Mater* 2010,58,6421–6430.
- [178] Schobel M, Altendorfer W, Degischer HP, Vaucher S, Buslaps T, Michiel MD, Hofmann M. *Compos Sci Tech* 2011,71, 724–733.
- [179] Porter GA, Liaw PK, Tiegs TN, Wu KH. *Mater Sci Eng A* 2001, 314,186–193.
- [180] Qian LH, Wang ZG, Toda H, Kobayashi T. *Mater Sci Eng A* 2003,357, 240-247.
- [181] Klaska AM, Beck T, Wannera A, Lohe D. *Mater Sci Eng A* 2009, 501, 6–15.
- [182] Huang YD, Hort N, Dieringa H, Maier P, Kainer KU. *Int J Fatigue* 2006, 28, 1399–1405.
- [183] Minaka M, Ceschini L, Boromei I, Ponte M. *Int J Fatigue* 2010, 32,218–226.
- [184] Chung DDL. *Appl Therm Eng* 2001, 21, 1593-1605.
- [185] Ruch PW, Beffort O, Kleiner S, Weber L, Uggowitzer PJ. *Compos Sci Tech* 2006, 66, 2677–2685.
- [186] Schobel M, Altendorfer W, Degischer HP, Vaucher S, Buslaps T, Michiel MD, Hofmann M. *Compos Sci Tech* 2011,71,724–733.
- [187] Gui M, Kang SK, Euh K. *Scripta Mater* 2005, 52, 51–56.
- [188] Qu XH, Zhang L, Wu M, Ren SB. *Prog Nat Sci* 2011,21,189–197.
- [189] Chu K, Jia C, Liang X, Chen H, Gao W, Guo H. *Mater Des* 2009,30,4311–4316.
- [190] Raj R, Saha A, An L, Hasselman DPH, Ernst P. *Acta Mater* 2002, 50, 1165–1176.
- [191] Molina JM, Narciso J, Weber L, Mortensen A, Louis E. *Mater Sci Eng A* 2008,480,483–488.
- [192] Chu K, Jia C, Tian W, Liang X, Chena H, Guo H. *Mater Des* 2009,30,3497–3503.
- [193] Chu K, Jia C, Tian W, Liang X, Chena H, Guo H. *Composites: Part A* 2010,41,161–167.
- [194] Lee JM, Lee SK, Hong SJ, Kwon YN. *Mater Des* 2012, 37,313–316.

- [195] Kady OE, Fathy A. *Mater Des* 2014, 54,348–353.
- [196] Couturier R, Ducret D, Merle P, Disson JP, Joubert P. *J Eur Cer Soc* 1997,17,1861-1866.
- [197] Mizuuchi K, Inoue K, Agari Y, Nagaokaa T, Sugioka M, Tanaka M, Takeuchi T, Tani J, Kawahara M, Makinoc Y, Ito M. *Composites: Part B* 2012,43,1557–1563.
- [198] Tatar T, Ozdemir N. *Physica B* 2010, 405,896–899.
- [199] Hochengap H, Yenb SB, Ishihara T, Yen BK. *Composites Part A* 1997, 28, 883-890.
- [200] Wang TC, Fan TX, Zhang D, Zhang GD, Xiong DS. *Mater Lett* 2007, 61, 1849–1854.
- [201] Bakshi SR, Patel RR, Agarwal A. *Comp Mater Sci* 2010, 50,419–428.
- [202] Xue C, Yu JK, Zhu XM. *Mater Des* 2011, 32, 4225–4229.
- [203] Fukuchi K, Sasaki K, Katagiri K, Imanishi T, Kakitsuji A. *Proc Eng* 2011,10,912–917.
- [204] Prieto R, Molina JM, Narciso J, Louis E. *Composites: Part A* 2011, 42, 1970–1977.
- [205] Zhu C, Ma N, Jin Y, Bai H, Ma Y, Lang J. *Mater Des* 2012,41,208–213.
- [206] Wu J, Zhang H, Zhang Y, Wang X. *Mater Des* 2012,41,344–348.
- [207] Wu J, Zhang H, Zhang Y, Li J, Wang X. *Mater Des* 2012,39,87–92.
- [208] Chen JK, Huang IS. *Composites: Part B* 2013, 44,698–703.
- [209] Monje IE, Louis E, Molina JM. *Composites: Part A* 2013, 48, 9–14.
- [210] Tan Z, Li Z, Fan G, Kai X, Ji G, Zhang L, Zhang D. *Diam Relat Mater* 2013, 31, 1–5.
- [211] Xue X, Yu JK. *Surf Coat Tech* 2013, 217, 46–50.
- [212] Shin Z, Yang W, Wang J, Liu G, Qiaon G, Jin Z. *Ceram Int* 2013,39,3365–3370.
- [213] Tan Z, Li Z, Xiong DB, Fan G, Ji G, Zhang D. *Mater Des* 2014, 55,257–262.
- [214] Mizuuchi M, Inoue K, Agari Y, Morisada Y Sugioka M, Tanaka M, Takeuchi T, Tani J, Kawahara M, Makino Y. *Composites: Part B* 2011,42,825–831.
- [215] Molina JM, Rheome M, Carron J, Weber L. *Scripta Mater* 2008,58,393–396.

[216] Tan Z, Li Z, Fan G, Guoa Q, Kai X, Ji G, Zhang L, Zhang D. *Mater Des* 2013,47,160–166.

Figure Captions

Fig. 1: Bright field TEM image showing dislocation tangles in the matrix of the as rolled Al-SiC composite.

Fig. 2: Bar charts depicting the damages caused by thermal cycling in the Al alloy-SiC, Al-SiC and Al-TiC composites against the number of cycles of heating and water quenching.

Fig. 3: Elongations for various test conditions and material systems.

Fig. 4: Longitudinal cross sections of (a) AlSi₇/SiC_p/10vol% and (b) AlSi₇/SiC_p/20vol% thermally cycled samples tested at 5–14 MPa, showing cavities, cracks and interfacial debonding (ID).

Fig. 5: Temperature dependence of relative linear length change (a) and CTE (b) for the composite and unreinforced matrix.

Fig. 6: SEM micrographs showing (a) crack initiation. (b) Propagation of thermal fatigue crack from notch tip in 65vol% SiC reinforced composite. (c) Propagation of thermal fatigue crack in 35 vol% SiC reinforced composite.